

Control of the pattern-recognition receptor EFR by an ER protein complex in plant immunity

Vladimir Nekrasov^{1,5}, Jing Li^{1,5,6}, Martine Batoux¹, Milena Roux¹, Zhao-Hui Chu^{1,7}, Severine Lacombe^{1,8}, Alejandra Rougon¹, Pascal Bittel², Marta Kiss-Papp², Delphine Chinchilla², H Peter van Esse³, Lucia Jorda⁴, Benjamin Schwessinger¹, Valerie Nicaise¹, Bart PHJ Thomma³, Antonio Molina⁴, Jonathan DG Jones¹ and Cyril Zipfel^{1,*}

¹The Sainsbury Laboratory, Norwich Research Park, Norwich, UK, ²Basel-Zurich-Plant Science Center, Botanical Institute, University Basel, Basel, Switzerland, ³Laboratory of Phytopathology, Wageningen University, Wageningen, The Netherlands and ⁴Centro de Biotecnología Genómica Plantas, ETSI Montes, Ciudad Universitaria s/n, Madrid, Spain

In plant innate immunity, the surface-exposed leucine-rich repeat receptor kinases EFR and FLS2 mediate recognition of the bacterial pathogen-associated molecular patterns EF-Tu and flagellin, respectively. We identified the Arabidopsis stromal-derived factor-2 (SDF2) as being required for EFR function, and to a lesser extent FLS2 function. SDF2 resides in an endoplasmic reticulum (ER) protein complex with the Hsp40 ERdj3B and the Hsp70 BiP, which are components of the ER-quality control (ER-QC). Loss of SDF2 results in ER retention and degradation of EFR. The differential requirement for ER-QC components by EFR and FLS2 could be linked to N-glycosylation mediated by STT3a, a catalytic subunit of the oligosaccharyltransferase complex involved in co-translational N-glycosylation. Our results show that the plasma membrane EFR requires the ER complex SDF2–ERdj3B–BiP for its proper accumulation, and provide a demonstration of a physiological requirement for ER-QC in transmembrane receptor function in plants. They also provide an unexpected differential requirement for ER-QC and N-glycosylation components by two closely related receptors.

The EMBO Journal (2009) 28, 3428–3438. doi:10.1038/emboj.2009.262; Published online 17 September 2009

Subject Categories: proteins; plant biology

Keywords: EFR; ER-quality control; pathogen-associated molecular patterns; pattern-recognition receptor; SDF2

*Corresponding author. The Sainsbury Laboratory, Norwich Research Park, Colney Lane, Norwich, NR4 7UH, UK. Tel.: +44 0 1603 450056; Fax: +44 0 1603 450011; E-mail: cyril.zipfel@tsl.ac.uk

⁵These authors contributed equally to this work

⁶Present address: Viikki Biocenter, Department of Biological and Environmental Sciences, Division of Genetics, University of Helsinki, POB 56, FIN-00014, Helsinki, Finland

⁷Present address: College of Plant Protection, Shandong Agricultural University, Taian, Shandong 271018, China

⁸Present address: INRA-UR 1052 Génétique et Amélioration des Fruits et Légumes, 84143 Montfavet Cedex, France

Received: 18 June 2009; accepted: 10 August 2009; published online: 17 September 2009

Introduction

Plants initially sense microbes through perception of pathogen (or microbe)-associated molecular patterns (PAMPs/MAMPs) by pattern-recognition receptors (PRRs) located on the cell surface leading to PAMP-triggered immunity (PTI) (Jones and Dangl, 2006; Zipfel, 2008). *Arabidopsis thaliana* detects a variety of PAMPs including fungal chitin, and bacterial flagellin and EF-Tu, or their peptide surrogates flg22 and elf18, respectively (Gomez-Gomez and Boller, 2000; Zipfel *et al*, 2006). Although recognition of fungal chitin and of an unknown bacterial PAMP depend on CERK1, a LysM domain receptor kinase (LysM-RK) (Miya *et al*, 2007; Wan *et al*, 2008; Gimenez-Ibanez *et al*, 2009), the related leucine-rich repeat receptor kinases (LRR-RKs) FLS2 and EFR are the PRRs for flagellin and EF-Tu, respectively. The LRR-RK BAK1 is rapidly recruited by FLS2 in a ligand-dependent manner to initiate downstream signalling (Chinchilla *et al*, 2007; Heese *et al*, 2007). Flagellin and EF-Tu recognition leads to MAP kinase activation, defence gene induction, production of reactive oxygen species in an oxidative burst, callose deposition, synthesis of the defence hormone salicylic acid (SA) and seedling growth inhibition (SGI) (Schwessinger and Zipfel, 2008). PAMP treatment leads to enhanced resistance to adapted pathogens (Zipfel *et al*, 2004, 2006; Ferrari *et al*, 2007), whereas defects in PAMP recognition lead to enhanced susceptibility to adapted and non-adapted pathogens (Zipfel *et al*, 2004, 2006; de Torres *et al*, 2006; Hann and Rathjen, 2007), showing a contribution of PTI to both basal and non-host resistance. Pathogenic virulence effectors evolved to directly target PRRs and their associated proteins to cause disease (Göhre *et al*, 2008; Shan *et al*, 2008; Xiang *et al*, 2008; Gimenez-Ibanez *et al*, 2009), further showing the importance of PTI for plant innate immunity.

FLS2 and EFR are transmembrane glycoproteins that need to transit through the secretory pathway to mature and reach their final destination at the plasma membrane. After translocation into the endoplasmic reticulum (ER), newly synthesised polypeptides interact with different chaperones that will assist them to fold properly and to avoid aggregation in a process called ER-quality control (ER-QC) (Anelli and Sitia, 2008). Unfolded proteins are retained in the ER until they are properly folded, or ultimately destroyed by ER-associated degradation (ERAD) in the cytosol (Vembar and Brodsky, 2008). Most of our knowledge on ER-QC is based on studies in yeast and mammals, while plant ER-QC mechanisms are still not well characterized (Vitale and Boston, 2008). Studies in mammals and yeast revealed that ER-QC relies on three main different pathways. The first, is specific to glycoproteins and depends on the folding sensor UDP-glucose:glycoprotein glucosyltransferase (UGGT) plus the lectins calnexin (CNX) and calreticulin (CRT) (Williams, 2006). The second relies on retention of misfolded proteins by the luminal-binding protein BiP, a member of the Hsp70 family of chaperones. In this system, the ER-localised co-chaperone Hsp40 protein ERdj3

first directly binds to the misfolded substrate. ERdj3 then recruits BiP and activates BiP ATPase activity present in its N-terminus, leading to interaction of the C-terminal region of BiP with the substrate and the release of ERdj3b (Jin *et al*, 2008, 2009). The BiP retention system acts independently of, or subsequent to, the CNX/CRT cycle (Buck *et al*, 2007). The third system involves the formation of disulfide bonds between free thiol groups in non-native proteins by protein disulfide isomerases and thiol oxidoreductases (Reddy *et al*, 1996; Anelli *et al*, 2003, 2007).

Despite the major contribution of PTI to plant innate immunity, our knowledge of the molecular events underlying PRR biogenesis, PAMP perception by PRRs, and downstream signalling is limited. We report here on an ER protein complex comprising stromal-derived factor-2 (SDF2), ERdj3B and BiP required for the proper biogenesis of the PRR EFR, and reveal an unexpected differential requirement of EFR and FLS2 for ER-QC and glycosylation components.

Results and discussion

Identification of *sdf2* mutants in a forward-genetic screen for Arabidopsis *elf18*-insensitive mutants

To identify new regulators of EFR function in Arabidopsis, we used the property of *elf18* to cause SGI (Zipfel *et al*, 2006) (Figure 1A) and screened ~35 000 T-DNA activation-tagging transgenic lines and ~137 500 ethyl methane sulphonate (EMS)-mutagenised M2 seeds (all in Col-0 background). We identified 160 *elf18*-insensitive (*elfin*) mutants. Sequencing

the *EFR* locus in these mutants identified 57 *efr* mutants corresponding to 37 different alleles (data not shown).

We isolated three allelic *elfin* mutants at a new locus by screening the activation-tagging transgenic population. Genetic analyses indicated that the mutation is recessive, suggesting that the phenotype is conferred by a loss-of-function mutation. All three mutants carried the same T-DNA insertion at the At2g25110 locus encoding the Arabidopsis orthologue of the murine stromal cell-derived factor-2 gene, *AtSDF2*, and were therefore named *sdf2-1* (Figure 1B–D; Supplementary Figure 1). In addition, an independent homozygous T-DNA insertion line (SALK_141321), *sdf2-2*, and two further *sdf2* alleles identified in the EMS *elfin* collection by DNA sequencing (*sdf2-3* and *sdf2-4*) were similarly impaired in *elf18*-triggered SGI (Figure 1B–D; Supplementary Figure 1). No developmental or growth defects were observed in the *sdf2* mutants under our growth conditions (data not shown). Finally, transgenic *sdf2-2* seedlings expressing the SDF2–3xHA fusion protein under the control of the *SDF2* promoter regained *elf18* sensitivity (Figure 1D; Supplementary Figure 1), showing that mutation in *SDF2* is responsible for the observed *elfin* phenotype.

AtSDF2 is a single copy gene in Arabidopsis and clear orthologs exist in all eukaryotes, except fungi (Supplementary Figure 2). Although *SDF2* is highly conserved in eukaryotes, no mutant phenotype has been reported in any organism so far. *AtSDF2* is a small protein of 218 amino acids (24 kDa) consisting of a 23 amino-acid (aa) predicted N-terminal signal peptide (SP) and three repeats of the MIR domain (Figure 1C) found in mannosyltransferases, the

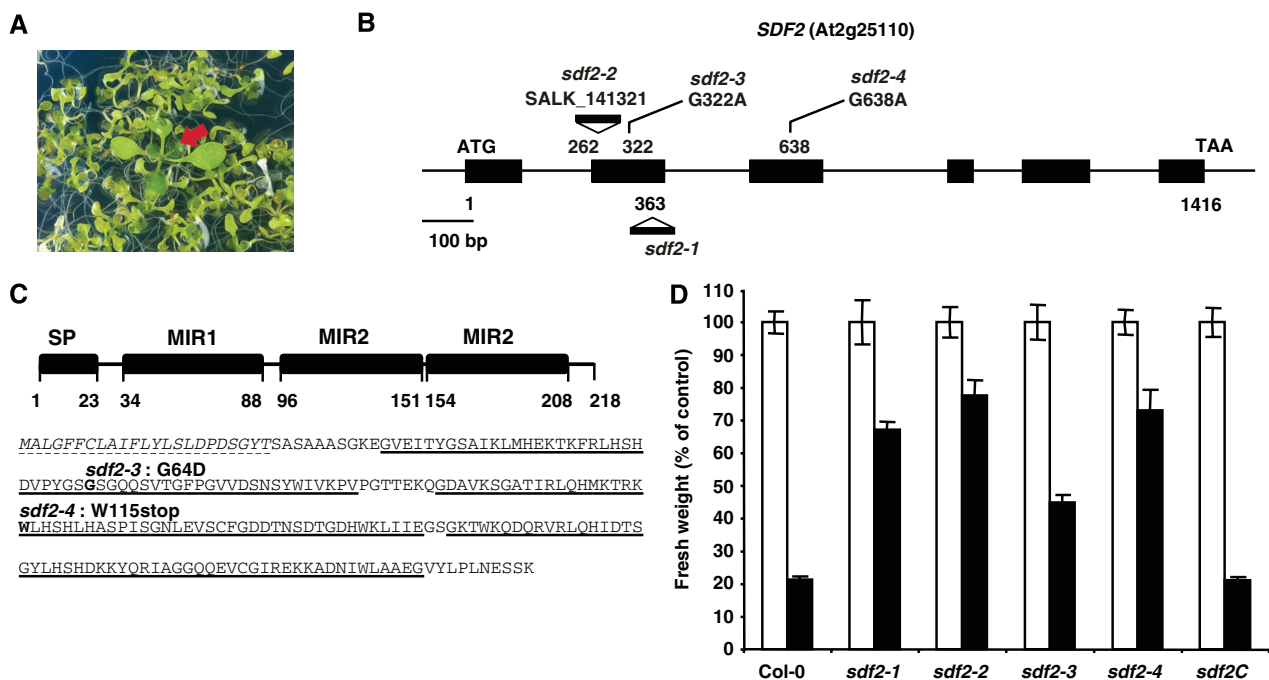


Figure 1 Identification of *sdf2* mutants. (A) Growth phenotype of *elfin* (*elf18*-insensitive) seedlings. Five-day-old Arabidopsis seedlings were covered with liquid MS medium containing 1% sucrose (MS 1%) supplemented with 50 nM *elf18* peptide. Seedling growth inhibition was scored qualitatively 1 week after treatment. The red arrowhead indicates an *elfin* mutant. (B) Schematic representation of the *SDF2* gene (At2g25110) with positions of the T-DNA insertions and point mutations. Exons are depicted as black boxes. (C) SDF2 protein organisation. Top, schematic representation of *SDF2* with the predicted signal peptide (SP) and MIR domains represented as black boxes. Bottom, *SDF2* protein sequence. SP, dashed underlines; MIR domains, underlined. The positions of the *sdf2* EMS alleles are indicated in bold. (D) Seedling growth inhibition triggered by *elf18* in wild type (Col-0) and *sdf2* alleles. Five-day-old Arabidopsis seedlings were transferred to liquid MS 1% without (white bars) or with 100 nM *elf18* (black bars). Seedling fresh weight was quantified 1 week after treatment. *Sdf2C* corresponds to *sdf2-2/SDF2p::SDF2-3xHA*. Results are average \pm s.e. ($n = 6$). Similar results were observed in at least three independent experiments.

inositol-3-phosphate receptor (IP3R) and the ryanodine receptor (RyR) (Ponting, 2000). Although many eukaryotic proteins contain MIR domains, SDF2 is the only MIR domain-containing protein in plants.

Loss of SDF2 strongly affects EFR function

As SDF2 is required for elf18-triggered SGI, we tested whether it is involved in other PTI responses. We first tested whether *sdf2-2* was also impaired in the flg22-triggered SGI. Flg22 sensitivity over a range of concentrations was slightly reduced in *sdf2-2* seedlings as compared with wild type in this assay, but to a lesser extent than with elf18 (Figure 2A). Elf18 and flg22 typically induce an oxidative burst and MAP kinase activation within minutes of treatment in wild-type plants (Figure 2B and C). Although the oxidative burst induced by elf18 was strongly diminished in *sdf2-2* leaves, it was less reduced after flg22 treatment (Figure 2B). In contrast, the oxidative burst triggered by the fungal PAMP chitin, which depends on the LysM-RK CERK1 (Miya *et al*, 2007; Wan *et al*, 2008), was not impaired at all in *sdf2-2* mutants (Figure 2B), indicating that SDF2 is not required for chitin responses. Activation of MAP kinases 4 and 6 (MPK4 and MPK6) was almost completely abolished after elf18 treatment, whereas weakly decreased in response to flg22 in *sdf2-2* seedlings, when compared with wild type (Figure 1C).

Loss of SDF2 leads to enhanced disease susceptibility to bacteria and fungi

Next, we tested whether *SDF2* is required for innate immunity. First, we compared the ability of elf18 and flg22 to

induce resistance to the virulent bacterial strain *Pseudomonas syringae* pv. *tomato* DC3000 (*Pto* DC3000). Elf18- and flg22-induced resistances were both reduced in *sdf2-2* leaves compared with wild type (Supplementary Figure 3). Spray-inoculated *fls2c* mutant plants are more susceptible to *Pto* DC3000 than wild type, whereas *efr-1* plants are not (Figure 3A). *Sdf2-2* plants were however hyper-susceptible to *Pto* DC3000, comparably to *fls2c* plants (Figure 3A). PTI defects can be subtle, but can be detected more sensitively with weakly virulent bacterial strains lacking effector molecules. The bacterial effectors AvrPto and AvrPtoB directly target FLS2, EFR and BAK1 to suppress PTI (Göhre *et al*, 2008; Shan *et al*, 2008; Xiang *et al*, 2008), whereas the phytotoxin coronatine (COR) suppresses PAMP-induced stomatal closure, allowing bacterial entry into the leaf apoplast (Melotto *et al*, 2006). When spray-inoculated, both *Pto* DC3000 *COR*⁻ and *Pto* DC3000 Δ *avrPto*/ Δ *avrPtoB* strains caused reduced disease symptoms and multiplied less than *Pto* DC3000 on wild-type plants (~1 and 2 log units, respectively) (Figure 3B and C). However, Arabidopsis *efr-1*, *fls2c* and *fls2c efr-1* mutants displayed more severe disease symptoms and allowed more bacterial growth when spray-infected with these strains (Figure 3B and C), especially in the case of *Pto* DC3000 Δ *avrPto*/ Δ *avrPtoB* that grew almost as much as *Pto* DC3000 in these lines (Figure 3C). We sometimes observed that *efr-1* and *fls2c efr-1* were more susceptible to *Pto* DC3000 strains compared with wild type and *fls2c*, respectively (data not shown), suggesting that FLS2 and EFR can act additively in perception of this bacterium. We found that, although *sdf2-2* plants were not substantially

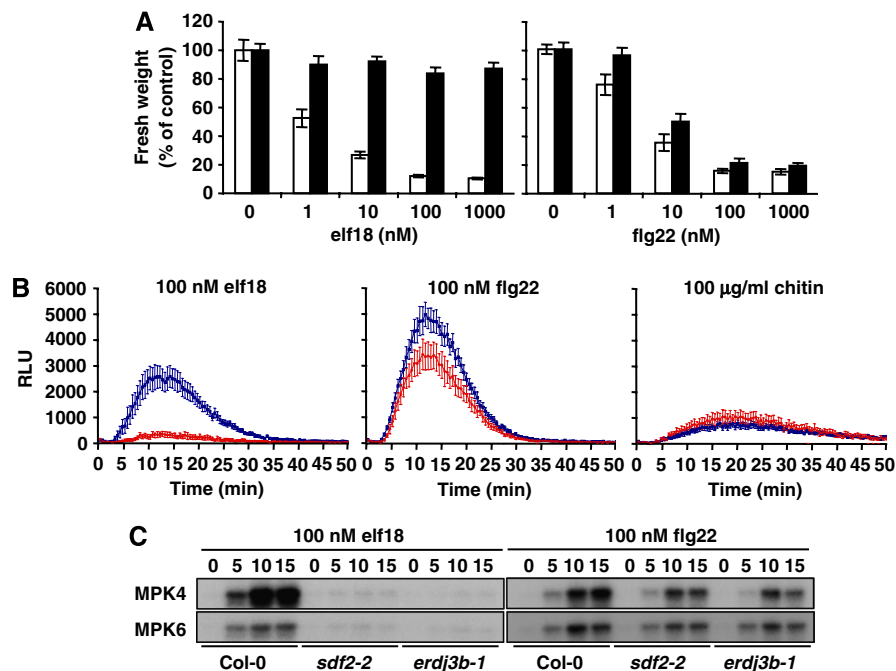


Figure 2 *Sdf2* mutant is compromised in PTI responses triggered by elf18 and, to a certain extent, flg22. (A) Seedling growth inhibition triggered by elf18 or flg22 in wild-type Col-0 (white bars) and *sdf2-2* (black bars) seedlings. Five-day-old Arabidopsis seedlings were transferred to liquid MS 1% supplemented with the indicated concentrations of peptides. Seedling fresh weight was quantified 1 week after treatment. Results are average \pm s.e. ($n = 6$). (B) Oxidative burst triggered by 100 nM elf18, 100 nM flg22 or 100 mg/ml chitin in wild-type Col-0 (blue) and *sdf2-2* (red) leaf discs measured in relative light units (RLU). Results are average \pm s.e. ($n = 12$). (C) Activation of the MAP kinases MPK4 and MPK6 in response to 100 nM elf18 or 100 nM flg22 in Col-0, *sdf2-2* and *erdj3b-1* seedlings (2 weeks old). Two-week-old Arabidopsis seedlings in liquid MS 1% were treated with 100 nM elf18 or flg22. Seedlings were flash frozen in liquid nitrogen at time points indicated. MPK4 and 6 were affinity purified using specific antibodies and used for *in vitro* kinase reactions performed with the myelin basic protein (MBP) as a substrate in the presence of [γ -³²P]ATP.

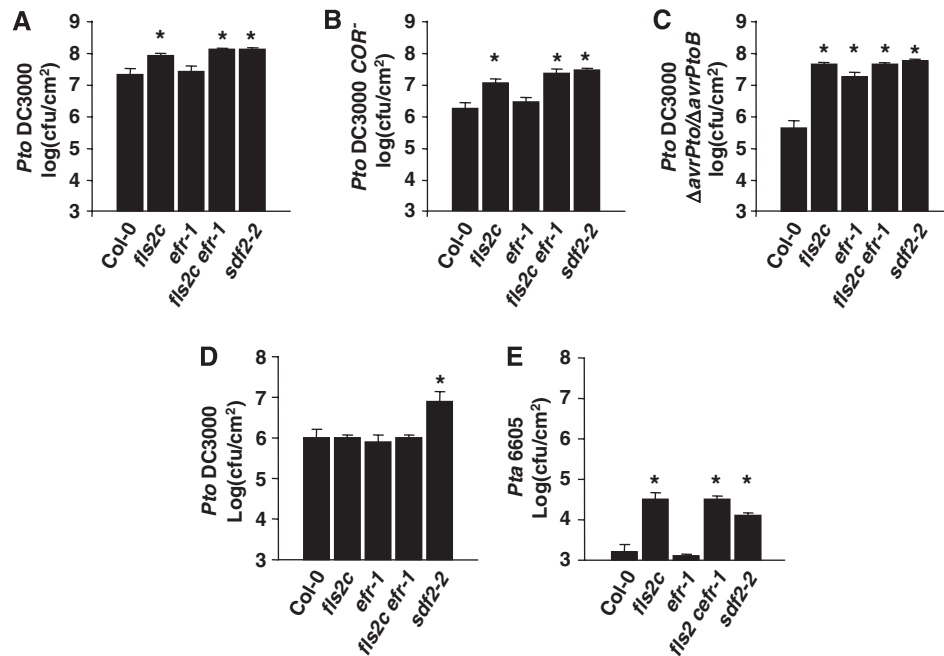


Figure 3 *Sdf2* mutant is more susceptible to bacterial pathogens. (A–C) Pre-invasive bacterial susceptibility assay. Five-week-old Col-0, *fls2c*, *efr-1*, *fls2c efr-1* and *sdf2-2* plants were sprayed with *Pseudomonas syringae* pv. *tomato* (*Pto*) DC3000 (A), *Pto* DC3000 *COR*[−] (B) or *Pto* DC3000 Δ *avrPto*/ Δ *avrPtoB* (C) (OD₆₀₀ of 0.02, supplemented with 0.04% Silwett L-77) and covered for the remaining of the experiment. Bacterial counts were assessed at 3 dpi. Results are average \pm s.e. ($n = 8$). (D, E) Post-invasive bacterial susceptibility assay. Leaves of 5-week-old plants were infiltrated with *Pto* DC3000 (OD₆₀₀ = 0.0002) (D) or *Pseudomonas syringae* pv. *tabaci* (*Pta*) 6605 (OD₆₀₀ = 0.002) (E). Bacterial populations were determined at 3 dpi. Results are average \pm s.e. ($n = 4$). For all above experiments, similar results were observed in at least three independent experiments and asterisks indicate $P < 0.05$ by *t*-test.

affected in their *flg22* responses (Figure 2), they were hyper-susceptible to both *Pto* DC3000 *COR*[−] and *Pto* DC3000 Δ *avrPto*/ Δ *avrPtoB* to a similar level as *fls2c efr-1* (Figure 3B and C). *Fls2* and *efr* mutants do not display enhanced susceptibility to *Pto* DC3000 when infiltrated into the leaves (Zipfel *et al*, 2004, 2006). Unexpectedly, we observed that *sdf2-2* was however more susceptible to *Pto* DC3000 after this infection procedure (Figure 3D). FLS2, but not EFR, is involved in the non-host resistance to the non-adapted bacterial strain *Pseudomonas syringae* pv. *tabaci* 6605 (Li *et al*, 2005) (Figure 3E). Surprisingly, we found that the *sdf2-2* mutation allowed growth of this strain to similar levels as on *fls2c* and *fls2c efr-1* plants (Figure 3E). Therefore, our results clearly show that *sdf2* mutants are more susceptible to bacterial infection than *efr* mutants.

We tested whether the enhanced disease susceptibility of *sdf2-2* could result from a defect in SA signalling, as SA positively regulates resistance to *Pseudomonas*, and as the *SDF2* gene was identified earlier as a potential direct target of the SA signalling regulator NPR1 (Wang *et al*, 2005). *SDF2* was however not required for secretion of the PR1 protein (a marker of NPR1-mediated responses) and bacterial resistance induced by the SA analogue benzothiadiazole (BTH) (Supplementary Figure 4). Thus, the hyper-susceptibility of *sdf2-2* plants to bacteria is not due to a defect in SA-mediated resistance. *SDF2* was also not required for the immunity triggered by recognition of the bacterial effectors AvrRpt2 and AvrRps4 (Supplementary Figure 5). Although *sdf2-2* was not affected in chitin sensitivity, we tested its susceptibility to fungal pathogens. Notably, *sdf2-2* was more susceptible to the virulent necrotrophic fungi *Alternaria brassicicola* and *Plectosphaerella cucumerina* (Figure 4). Thus, *SDF2* is

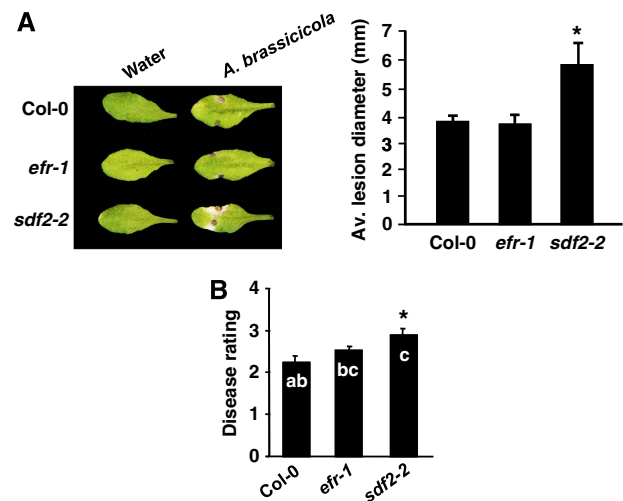


Figure 4 *Sdf2* mutant is more susceptible to fungal pathogens. (A) Susceptibility to *A. brassicicola*. Left, macroscopic symptoms and disease rating at 5 dpi. Right, lesion diameter at 5 dpi. Similar results were observed in four independent experiments and asterisks indicate $P < 0.05$ by one-way ANOVA with Bonferroni post hoc test. (B) Susceptibility to *P. cucumerina*. Left, macroscopic symptoms 14 dpi. Right, average disease rating (DR \pm s.d.) of the indicated genotypes at 14 dpi. DR varies between 0 (no symptoms) and 5 (dead plants). Letters indicate $P \leq 0.05$ by ANOVA with Bonferroni post hoc test. Data are from one of two independent experiments that gave similar results.

required for EFR, and to a lesser extent for FLS2, function. In addition, the enhanced disease susceptibility phenotype of *sdf2-2* to bacteria and fungi suggests that *SDF2* may have an important function in regulating other, yet unknown, PRRs

involved in bacterial and fungal recognition, or conceivably other components of plant defence.

SDF2 localises to the ER in a complex with ERdj3B and BiP

Plant SDF2 proteins contain a predicted SP, but no ER or Golgi retention signals, whereas SDF2 proteins from other eukaryotes carry a C-terminal K/HDEL motif (Supplementary Figure 2) classically associated with the retention of soluble proteins in the ER. To localise AtSDF2 within the plant cell, we transiently co-expressed AtSDF2-eYFP fusion protein under the control of its native promoter with the ER marker ER-CK (35S::CFP-HDEL) (Nelson *et al*, 2007) in *Nicotiana benthamiana*. Confocal microscopy revealed overlapping ER localisation for both expressed proteins (Figure 5A). The same ER localisation pattern was observed in *sdf2-2* plants transgenic for *AtSDF2p::SDF2-eYFP* (Figure 5B), suggesting that SDF2 localises to the ER.

As SDF2 does not possess an ER retention signal, its ER localisation could be due to its interaction with ER resident proteins. To test this hypothesis, we searched for SDF2 interactors *in planta*. Immunoprecipitation of proteins associated with SDF2-3xHA and subsequent mass spectrometry analysis revealed the soluble luminal protein ERdj3B (At3g62600) as the major SDF2 interactor (Supplementary Figure 6). ERdj3B, an ER-localised member of the HSP40

co-chaperone family, is one of the two Arabidopsis orthologs of the mammalian ERdj3 and yeast Scj1p proteins (Yamamoto *et al*, 2008). The SDF2-ERdj3B interaction was confirmed *in planta* with a specific anti-ERdj3B antibody (Figure 5C). Although ERdj3B directly interacted with SDF2 in the yeast two-hybrid (Y2H) system, its Arabidopsis paralog ERdj3A did not (Figure 5D; Supplementary Figures 7 and 8). In mammals, SDF2L exists in complex with ERdj3 and the luminal-binding protein BiP, an ER-localised member of the HSP70 family of chaperones (Meunier *et al*, 2002; Bies *et al*, 2004; Jin *et al*, 2008). Similarly, we found that the SDF2 immunocomplex also contains BiP in Arabidopsis (Figure 5C). There are three BiP isoforms in Arabidopsis (BiP1-3) (Noh *et al*, 2003). In Y2H assays, BiP1-3 interacted with ERdj3B, as well as with ERdj3A, but not with SDF2 (Figure 5D; Supplementary Figure 7). These results indicate that, in Arabidopsis, SDF2 exists in a complex with ERdj3B and BiP1-3, in which ERdj3B may act as a bridge between SDF2 and BiP. Notably, SDF2 was not found in complex with other ER resident proteins under the conditions tested (Supplementary Figures 8 and 9), showing that the association of SDF2 with ERdj3B and BiP was specific. As both SDF2 and ERdj3B lack an ER retention signal, their ER localisation might be due to interaction with BiPs. Three *erdj3b* alleles were independently identified by map-based cloning and sequencing of *elfin* mutants (Figure 6A; Supplementary

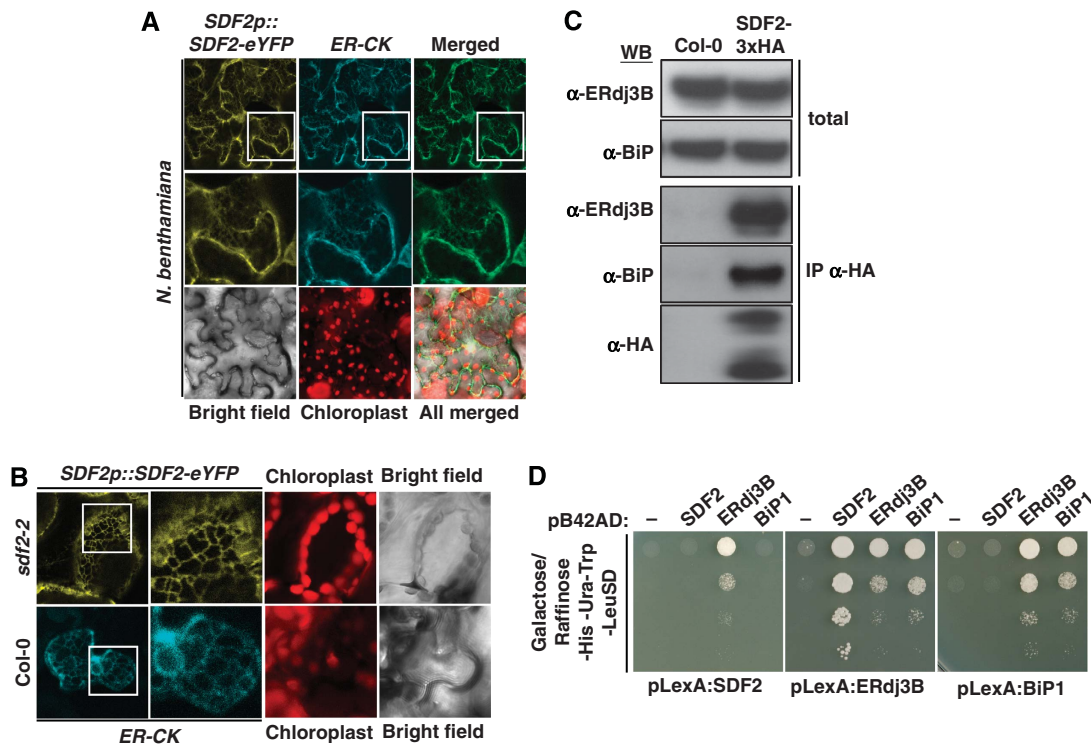


Figure 5 SDF2 exists in an ER complex with ERdj3b and BiP. (A) Subcellular localisation of SDF2 in *N. benthamiana*. The constructs *SDF2p::SDF2-eYFP* and ER-CK (35S::HDEL-CFP) were transiently co-expressed by Agrobacterium-mediated transformation in *N. benthamiana* leaves. Confocal analysis of transformed cells was performed at 2 dpi. The middle row of panels are zoom-ins. (B) Subcellular localisation of SDF2 in transgenic *sdf2-2/SDF2p::SDF2-eYFP* Arabidopsis leaves. The second column of panels corresponds to zoom-ins. (C) Co-immunoprecipitation of SDF2 with ERdj3B and BiP *in vivo*. Protein extract from *sdf2-2/SDF2p::SDF2-3xHA* or wild-type Col-0 seedlings were subjected to immunoprecipitation with anti-HA affinity matrix. Western blot analysis was performed with anti-ERdj3B, anti-BiP and anti-HA antibodies. (D) ERdj3B serves as an adaptor between SDF2 and BiP. Yeast cultures were grown overnight in the -His-Ura-Trp liquid SD medium supplemented with glucose. Cultures were spun down and resuspended in water to $OD_{600} = 1$. A series of 10-fold dilutions was plated on -His-Ura-Trp-Leu SD medium supplemented with galactose and raffinose to assess the expression of the LEU reporter gene. Images were taken after 3 days incubation at 30°C.

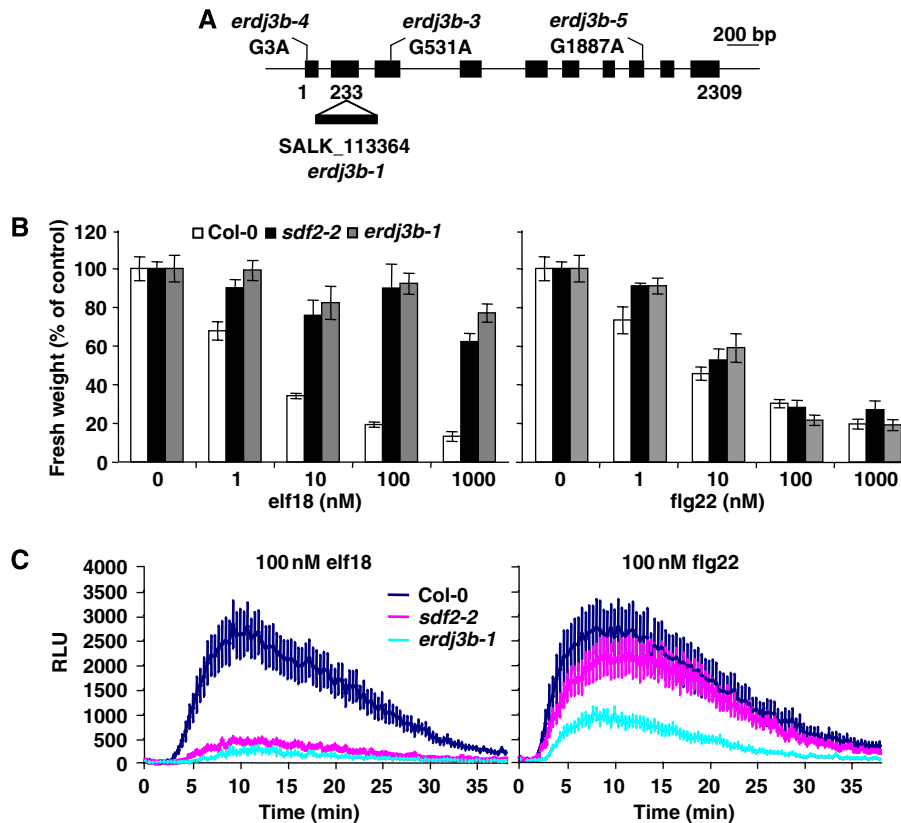


Figure 6 *Erdj3b* mutants show a phenotype similar to *sdf2*. (A) Schematic representation of the *ERdj3B* gene (At3g62600) with position of the T-DNA insertions and point mutations. Exons are depicted as black boxes. (B) Seedling growth inhibition triggered by elf18 or flg22 in wild-type Col-0 (white bars), *sdf2-2* (black bars) and *erdj3b-1* (grey bars). Results are average \pm s.e. ($n = 6$). (C) Oxidative burst triggered by 100 nM elf18 or 100 nM flg22 in wild-type Col-0 (blue), *sdf2-2* (purple) and *erdj3b-1* (cyan) leaf discs measured in relative light units (RLU). Results are average \pm s.e. ($n = 12$).

Figure 10). Analysis of a T-DNA null allele later confirmed that *erdj3b-1* plants were strongly affected in the elf18-triggered SGI, oxidative burst and MAP kinase activation, resembling *sdf2-2* plants (Figures 6B and C and 2C). *Erdj3b-1* was also weakly impaired in flg22 responses (Figures 6B and C and 2C) but not in chitin responses (Supplementary Figure 11). These results reveal that ERdj3B is also required for EFR and to a lesser extent FLS2 function.

The unfolded protein response (UPR) is activated by conditions that overload the ER-QC (Vembar and Brodsky, 2008; Vitale and Boston, 2008). Interestingly, we found that both *sdf2-2* and *erdj3b-1* were more sensitive to the drug tunicamycin, an inhibitor of N-glycosylation that triggers the UPR (Supplementary Figure 13), providing additional evidence for SDF2 and ERdj3B being involved in ER-QC. We also analysed functions for BiP1–3 in elf18 responses. Single *bip1*, *bip2* or *bip3* mutants all showed wild-type levels of elf18 responses (Supplementary Figure 12). Although the single *bip2* mutant was shown earlier to be fully impaired in SA-induced resistance (Wang *et al*, 2005), BiP1 and BiP2 are highly similar and might be functionally redundant, whereas BiP3 is more distantly related (Noh *et al*, 2003). We therefore generated a *bip1-1 bip2-1* double mutant, which showed a wild-type response to elf18 as well (Supplementary Figure 12). Silencing of all three Arabidopsis BiP genes recently proved to be lethal (Hong *et al*, 2008) thus preventing us from testing the possible requirement of all three BiPs in elf18 responses.

SDF2 is required for EFR biogenesis

On the basis of its association with ERdj3B and BiP, we hypothesised that SDF2 is also part of the ER-QC. We therefore tested whether SDF2 could regulate EFR directly. As *EFR* gene expression was not affected in *sdf2-2* (Supplementary Figure 14A), we next determined EFR protein levels *in vivo*. We generated *efr-1*, *sdf2-2* and *efr-1 sdf2-2* lines transgenic for the *EFRp::EFR-eGFP-HA* construct to enable detection of physiological levels of EFR protein. Expression of the tagged EFR complemented the *efr-1* mutation (data not shown) and we detected a single band running at ~ 175 kDa, the expected size for the glycosylated form of EFR-eGFP-HA in several independent primary transformants (Supplementary Figure 14B). However, the EFR protein level in total extracts was strongly reduced in the *efr-1 sdf2-2* and *sdf2-2* backgrounds (Supplementary Figure 14B; Figure 7A and B), showing a requirement of SDF2 for EFR protein accumulation. The enzyme endoglycosidase H (Endo H) cleaves off ER-specific glycans, whereas complex glycans that are matured during their transit through the Golgi apparatus are resistant to Endo H cleavage. Therefore, Endo H treatment allows the differentiation of plasma membrane localised glycoproteins from their ER localised counterparts. Using Endo H assays, we found that, although transgenic *sdf2-2* plants express some levels of EFR protein, it is completely cleaved by Endo H (Figure 7C), revealing that the expressed EFR protein is retained in the ER. In contrast, most of the EFR protein

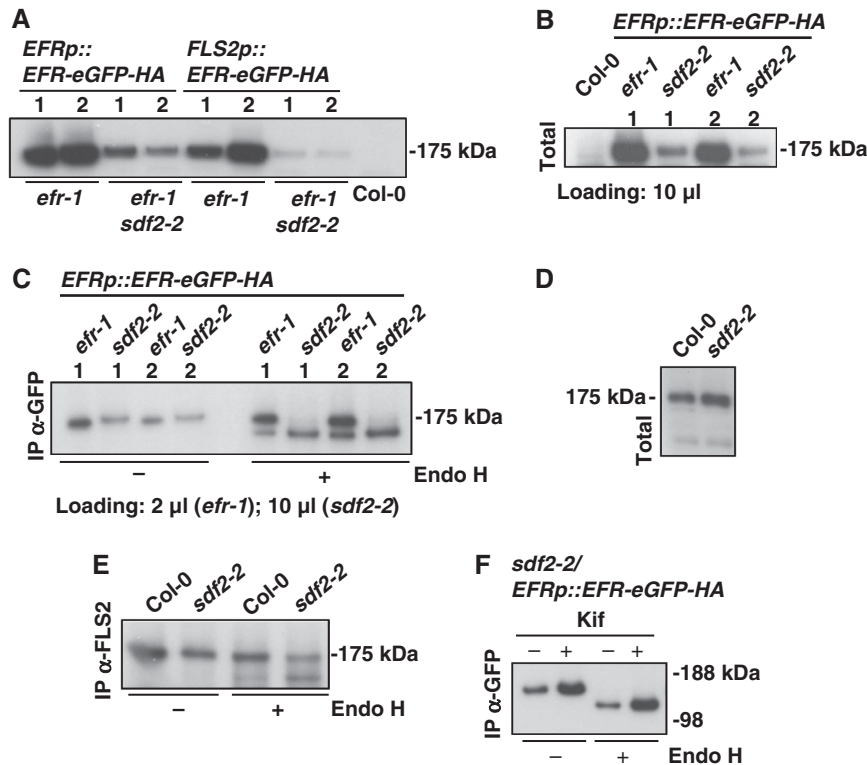


Figure 7 SDF2 controls EFR protein accumulation. (A) Effect of the *sdf2-2* mutation on EFR protein levels. Total protein extracts were prepared from T2 transgenic lines (the numbers above the lanes indicate independent lines). Col-0 was used as a negative control. Equal amounts of plant tissue were used in all cases. (B) Relative abundance of EFR expressed under its native promoter in *efr-1* and *sdf2-2* genetic backgrounds. (C) Effect of the *sdf2-2* mutation on EFR glycosylation state. Endo H assays were performed with the EFR protein from *efr-1/-* and *efr-1 sdf2-2/EFRp::EFR-eGFP-HA*. EFR was immunoprecipitated using anti-GFP agarose beads (Caltag Medsystems) and incubated with (+) or without (-) Endo H for 1 h at 37°C. (D) Immunoblot of FLS2. Total protein extracts were prepared from Col-0 and *sdf2-2* plants as described in (A). FLS2 was detected with a polyclonal anti-FLS2 antibody. (E) Effect of *sdf2-2* on the FLS2 glycosylation state. FLS2 was immunoprecipitated using the polyclonal anti-FLS2 antibody and protein G sepharose beads (Sigma). The Endo H assay was performed as in (C). (F) EFR expressed in the *sdf2-2* background is stabilised by kifunensine (Kif). Despite the increase in the protein level on treatment with Kif, EFR expressed in *sdf2-2* remains sensitive to Endo H. Two-week-old seedlings were incubated for 20 h in the 1/2 MS medium with (+) or without 50 μM Kif. The protein extracts were prepared as in (A) and the Endo H assay was performed as in (C). In (A–C, F) EFR was detected with the anti-GFP antibody (TP401, AMS Biotechnology).

expressed in the *efr-1* background is resistant to Endo H, revealing its localisation at the plasma membrane. Consistently, cross-linking and binding studies with radiolabelled elf18 peptide indicated that *sdf2-2* has fewer binding sites than wild type (Supplementary Figure 15A), corroborating the reduced elf18 sensitivity of the *sdf2-2* mutant (Figures 1 and 2). Although FLS2 accumulated to similar levels in *sdf2-2* and WT total extracts (Figure 7D), half of FLS2 seems to be retained in the ER in *sdf2-2* (Figure 7E). This is consistent with the decreased flg22 sensitivity and binding of *sdf2-2* (Figure 2A and B; Supplementary Figures 3 and 15).

Interestingly, treatment with kifunensine, an inhibitor of ER mannosidase I that prevents ER exit and consequently ERAD (Tokunaga *et al*, 2000), increased EFR protein levels in *sdf2-2* (Figure 7F), whereas the 26S proteasome inhibitor MG132 had no effect (Supplementary Figure 16). Despite increased levels after kifunensine treatment, Endo H assays revealed that EFR is still retained in the ER in the *sdf2-2* background (Figure 7F). These results revealed that EFR is actively degraded in *sdf2-2* and that this degradation occurs outside of the ER. Future work will be required to determine whether EFR is degraded in the cytosol as most ERAD substrates or in the vacuole as recently shown for a subset of plant ERAD substrates (Foresti *et al*, 2008).

EFR function specifically depends on SST3A-mediated N-glycosylation

An intriguing question is why FLS2 function is affected less than EFR by mutations in ER-QC components, whereas CERK1 function is not affected at all. This is particularly surprising as EFR and FLS2 are structurally similar and belong to the subfamily XII of LRR-RKs. One possible explanation for the apparent specificity could be due to a receptor level threshold required for responsiveness. EFR protein levels might be much lower than FLS2 protein levels. Therefore, mutations in ER-QC components would reduce EFR protein amounts to a level that severely impacts elf18 responses, whereas FLS2 protein amounts would still be sufficient to ensure flg22 responses. However, expression of EFR under the control of the FLS2 promoter in *efr-1* and *efr-1 sdf2-2* did not revert the reduced EFR accumulation because of the *sdf2* mutation (Figure 7A). Therefore, the requirement of SDF2 for EFR is not due to a decreased protein expression compared with FLS2, and might rather be due to intrinsic properties of EFR.

Notably, we have identified in our *elfin* population alleles of *STT3A* (*Staurosporin and temperature sensitive-3A*), coding for a component of the ER oligosaccharyltransferase (OST) complex involved in N-glycosylation of nascent

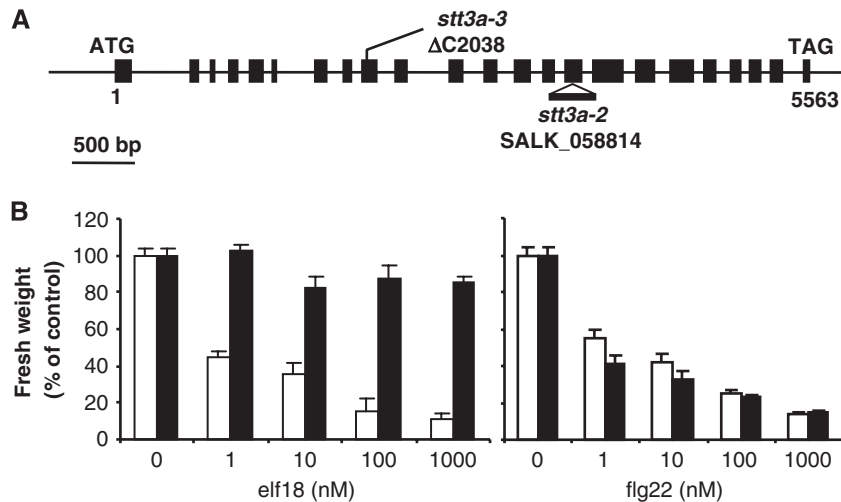


Figure 8 *Stt3a* affects EF-Tu but not flagellin responsiveness. (A) Schematic representation of the *STT3A* gene with positions of the single nucleotide deletion and the T-DNA insertion. Exons are depicted as black boxes. *stt3a-3* and *stt3a-2* (Koiwa *et al*, 2003) are indicated. (B) Seedling growth inhibition triggered by elf18 or flg22 in wild-type Col-0 (white bars) and *stt3a-2* (black bars) seedlings. Five-day-old Arabidopsis seedlings were transferred into liquid MS 1% supplemented with the indicated concentrations of peptides. Seedling fresh weight was quantified 1 week after treatment. Results are average \pm s.e. ($n = 6$).

proteins (Koiwa *et al*, 2003). Unexpectedly, the characterisation of *stt3a* mutants revealed that STT3a-mediated N-glycosylation is indispensable for EFR, but dispensable for FLS2 function (Figure 8; Supplementary Figure 17). Although plant extracts of *stt3a* mutants still contain glycosylated proteins, the pattern of N-glycosylation is different (Koiwa *et al*, 2003), suggesting that only a subset of proteins are STT3a substrates. In mammals, STT3a is important for co-translational N-glycosylation of nascent proteins, whereas STT3b rather has a function in post-translational N-glycosylation (Ruiz-Canada *et al*, 2009). Arabidopsis *stt3b* mutants were not affected in elf18- or flg22-triggered SGI (data not shown), showing that STT3A is the key glycosylation determinant for EFR. Although both EFR and FLS2 carry numerous putative glycosylation sites, they may have different glycosylation states (e.g. position, number of glycosylated sites, glycan structures) that could impact their interaction with and dependence on the ER-QC machinery.

A subset of ER-QC components is specifically required for the biogenesis of transmembrane PRRs

In addition to reporting a function for SDF2 and ERdj3B in plant innate immunity, we and others have found that the Arabidopsis CRT3 and UGGT are also required for EFR function, as loss of either CRT3 or UGGT leads to complete loss of EFR accumulation (Li *et al*, 2009; Saijo *et al*, 2009). Altogether, this shows that EFR relies on both the CNX/CRT3 and SDF2/ERdj3B/BiP systems for its proper function. BiP and CRT exist in an abundant large complex in tobacco (Denecke *et al*, 1995; Crofts *et al*, 1998). CRT3, SDF2, ERdj3B, BiP and potentially UGGT may therefore exist in the same complex to regulate proper EFR folding. Such large chaperone complexes have been reported in mammals (Meunier *et al*, 2002), but we have failed so far to detect CRT3 or UGGT in the SDF2 immunocomplex. Further work is therefore required to investigate the existence of such large complex.

Our infection data strongly suggest that SDF2 may also regulate other unknown PRRs involved in bacterial and fungal recognition, or conceivably other defence components, whose identity will be interesting to investigate in future experiments. The specificity of the reported mutations, however, show that SDF2 and ERdj3B are specifically involved in plant innate immunity and clearly argues against a general defect in protein secretion. It would be interesting to test whether they are also having a function in other stress responses, for example, abiotic stresses, and to identify which other members of the Hsp70 and Hsp40 families for example ensure folding of proteins involved in other plant physiological functions.

This work provides the first demonstration of a requirement for the ER-QC in generating functional transmembrane receptors in plants. Recent studies reported a function for the ER-QC in retaining mutant variants of the brassinosteroid receptor BRI1, a LRR-RK, within the ER (Jin *et al*, 2007; Hong *et al*, 2008). However, in these studies, the function of wild-type BRI1 was not affected by mutations in ER-QC components. This is in clear contrast with our findings that mutations in a subset of ER-QC components affect wild-type EFR.

Although most cytoplasmic nucleotide-binding domain and LRR-containing (NLR) immune receptors involved in effector recognition rely on the HSP90-SGT1 chaperone complex (Shirasu, 2009), we propose that a subset of surface-exposed PRRs, including EFR require one or several ER complexes comprising SDF2, ERdj3B, BiP and potentially CRT3 and UGGT for their accumulation and subcellular localisation. We speculate that as EFR is only found in the *Brassicaceae*, whereas FLS2 has been identified in several dicots and monocots (Takai *et al*, 2008; Zipfel, 2008), EFR may have evolved more recently than FLS2, and thus its amino-acid sequence is less capable of folding properly in the absence of ER-QC components. It is conceivable that evolution of new recognition specificities may result in proteins that detect novel ligands but that have not been selected for

high protein stability, and thus require extra “buffering” (Queitsch *et al*, 2002).

Materials and methods

Plant materials and growth

A. thaliana ecotype Columbia (Col-0) was the background for all mutants and transgenic lines used in this study. The Arabidopsis plants used in this study were grown as one plant per pot at 20–21°C with an 10 h photoperiod, or on plates containing MS salts medium (Duchefa), 1% sucrose, and 1% agar with a 16 h photoperiod.

The T-DNA insertion lines SALK_141321 (*sd2-2*), SALK_113364 (*erdj3b-1*), SALK_063999 (*bip1-1*), SALK_093564 (*bip1-2*), SALK_47956 (*bip2-1* gift from X Dong), *bip3-2*, GABI_075D06, and SALK_024133 (*bip3-1*) were obtained from the Nottingham Arabidopsis Stock Centre (Nottingham, UK). The *fls2c efr-1* double mutant was generated by crossing *fls2c* (Zipfel *et al*, 2004) with *efr-1* (Zipfel *et al*, 2006). Primers used to genotype the T-DNA lines are listed in Supplementary Table 1.

Elfin forward-genetic screen

To isolate *elf-18 insensitive (elfin)* plants, we screened ~35 000 T-DNA activation-tagging transgenic lines (Molinier *et al*, 2004) (gift from J Molinier) and ~137 500 EMS-mutagenised M2 seeds (Tedman-Jones *et al*, 2008) (all in Col-0 background). Five-day-old seedlings germinated on MS 1% agar plates were submerged with liquid MS 1% supplemented with 50 nM elf18. At 8 to 10 days after treatment, SGI was visually scored and putative *elfin* mutant plant was transferred to the soil. Progenies of ~300 putative *elfin* mutants were retested in the next generation by a quantitative SGI assay, as described in Zipfel *et al* (2006). At the end, 160 *elfin* mutants were confirmed, including 57 that carry mutations in *EFR*.

The genomic DNA flanking the T-DNA insertion in the *sd2-1* mutant was cloned using thermal asymmetric interlaced-PCR (TAIL-PCR), based on Liu *et al* (1995).

To identify the *erdj3b-3* mutation, *elfin* plants in the Columbia-0 (Col-0) background were crossed to wild-type plants of the Landsberg *erecta* (Ler-0) ecotype. Genomic DNA from *elfin* seedlings in the segregating F₂ population was extracted and used for subsequent PCR analysis. The mutation was mapped to chromosome III between the markers NGA6 and NGA112 using a set of known simple sequence length polymorphism markers (data not shown). Fine mapping delimited the mutation to a 51-kb interval between the cleaved amplified polymorphic sequence markers CHIII-23122 and CHI-23173. Sequencing the whole region in the mutant identified a single-nucleotide mutation in ERdj3B (At3g62600).

Generation of transgenic plants

SDF2p::SDF2-eYFP construct was generated by PCR amplification of the *SDF2* genomic fragment, including the promoter and the coding region, with 5'-CACCAAAATTAATTTCCATGATGATAAAATTA-3' and 5'-CTTGCTGCTCTCATTAAGGG-3' primers and resulting PCR product was cloned into the *pENTRY-D/TOPO* vector using the *pENTR* Directional TOPO Cloning Kit (Invitrogen). The resulting clone was sequenced and the insert transferred into the GATEWAY-compatible vector *pGWB40* (Nakagawa *et al*, 2007) using GATEWAY LR CLONASE II enzyme (Invitrogen). The final construct was electrotransformed into *Agrobacterium tumefaciens* strain GV3101.

SDF2p::SDF2-3xHA construct was generated by PCR amplification of the *SDF2* genomic fragment, including the promoter and the coding region, with 5'-TACAATTGAAAATTAATTTCCATGATGATAAAATTA-3' and 5'-GGATCCGAGACGCTTGCTGCTCTCATTAAGGG-3' primers. The resulting PCR product was cloned into the *pGEMTeasy* vector by the T/A ligation. The clone was sequenced. The insert was then released by digesting with *MfeI* and *BsmBI* and ligated into the *epiGreenB5* binary vector digested with *EcoRI* and *BamHI*. As a result, the *Pro35S::GUS* cassette in *epiGreenB5* was replaced with *SDF2p::SDF2* producing the *SDF2p::SDF2-3xHA* fusion.

EFRp::EFR-eGFP-HA construct has been generated as following: the genomic fragment comprising the *EFR* promoter plus the coding region was PCR-amplified from Col-0 genomic DNA using 5'-ATCCGGGATCTAGACGATTAAGTAATTGAG-3' and 5'-ATGGATCCCATAGTATGCATGTCCTGATTTTA-3' primers, and cloned into the *pGEMTeasy* vector by the T/A ligation. The resulting clone was

sequenced. The *EFRp::EFR* insert was further subcloned into the *epiGreenB(eGFP-HA)* vector: *pGEMTeasy:EFRp::EFR* clone was digested with *EcoRI* + *SacI* and *SacI* + *BamHI* in two separate reactions and the two released fragments of the insert were ligated into the *epiGreenB(eGFP-HA)* vector, digested with *EcoRI* and *BamHI*, using the three-way ligation method.

FLS2p::EFR-eGFP-HA construct has been generated as following: the *FLS2* promoter was PCR-amplified from Col-0 genomic DNA using 5'-ATCAATTGcccttttggacattctaataat-3' and 5'-CATGTCGATTA TAAAAAGATAAATCTATAGACGAAGTCATATGT-3'. The *EFR* 5'-UTR plus the coding region were PCR-amplified from Col-0 genomic DNA using 5'-Atgactctgtctatagattatctttttataatgcacatgaagc-3' and 5'-ATGGATCCCATAGTATGCATGTCCTGATTTTA-3' primers. A fusion between *FLS2p* and *EFR* was created using the chimeric PCR method and the resulting PCR fragment was cloned into the *pGEMTeasy* vector by the T/A ligation. The resulting clone was sequenced. The *FLS2p::EFR* insert was further subcloned into the *epiGreenB(eGFP-HA)* vector: *pGEMTeasy:FLS2p::EFR* clone was digested with *MfeI* + *BamHI* and the released insert was ligated into the *epiGreenB(eGFP-HA)* vector, digested with *EcoRI* and *BamHI*.

epiGreenB(eGFP-HA) was constructed as following: a PCR fragment comprising eGFP followed by a single HA tag (eGFP-HA) was cloned into the *pBin19g* vector (Rivas *et al*, 2004) using *BamHI* and *XbaI* restriction enzymes to replace the single HA tag with eGFP-HA in this vector. The resulting *pBin19(eGFP-HA)* vector was digested with *BamHI* and *HindIII* enzymes, and the released fragment containing eGFP-HA-NOS was cloned into the *epiGreenB5* vector using the same restriction enzymes. As a result, the 3xHA tag in *epiGreenB5* was replaced with eGFP-HA producing the *epiGreenB(eGFP-HA)* vector.

Both *epiGreenB(eGFP-HA):EFRp::EFR-eGFP-HA* and *epiGreenB5::SDF2p::SDF2-3xHA* constructs were electroporated into *A. tumefaciens* strain GV3101 carrying the *pSOUP* helper plasmid. All constructs were transformed into relevant Arabidopsis mutant lines using the floral dipping method (Clough and Bent, 1998). The transformants were selected on the MS agar medium supplemented with 10 µg/ml kanamycin in the case of *SDF2p::SDF2-eYFP* and spraying soil grown seedlings with BASTA in the case of *SDF2p::SDF2-3xHA* and *EFRp::EFR-eGFP-HA*.

PTI assays

SGI and oxidative burst assays were performed as described earlier (Zipfel *et al*, 2006) except that luminescence was measured using a Varioscan Flash plate reader. MAPK assays were performed as described (Meskiene *et al*, 2003) using antibodies against MPK4 and MPK6 (Sigma).

Infection assays

Bacterial assays were performed as described earlier (Zipfel *et al*, 2004). Inoculations with *A. brassicicola* and *P. cucumerina* were performed as described earlier (Hernández-Blanco *et al*, 2007; van Esse *et al*, 2008).

For the BTH-induced secretion of PR-1, intercellular wash fluid was collected as described earlier (Wang *et al*, 2005) from equal amounts of leaves treated for 24 h with water or BTH (300 µM). For BTH-induced resistance, water or BTH (300 µM; black bars) were sprayed onto leaves from 5-week-old plants 24 h before infiltrating *Pto* DC3000 (OD₆₀₀ = 0.0002). Bacterial populations were determined at 2 dpi.

Transient expression in *N. benthamiana*

A. tumefaciens strains were grown in L medium supplemented with appropriate antibiotics overnight. Next morning cultures were spun down and resuspended in 10 mM MgCl₂ to OD₆₀₀ = 0.6. *A. tumefaciens* strains carrying *ER-CK (pBin20:35S::CFP-HDEL)* and *pGWB40:SDF2p::SDF2-eYFP* were mixed 1:1 and syringe-infiltrated into 3-week-old *N. benthamiana* leaves. The confocal analysis was performed at 2 dpi.

Confocal microscopy

Analysis of intracellular fluorescence was performed by confocal laser-scanning microscopy on a Leica DM6000B/TCS SP5 confocal microscope (Leica Microsystems CMS GmbH, Germany) using a 20 × objective. Fluorophores were excited using an argon laser at 458 nm (CFP) or 514 nm (YFP). Images were collected in the

multi-channel mode and the overlay images were generated using the Leica analysis software LAS AF1.8.2.

Y2H assays

Y2H assays were performed using MATCHMAKER LexA two-hybrid system (Clontech). cDNAs encoding proteins tested were PCR amplified using specific primers. In all cases, the SP was omitted. The amplified PCR fragments were first cloned into the *pGEMTeasy* vector using the T/A ligation, sequenced and then subcloned, using restriction enzymes specified in the table, into *pLexA* and *pB42AD* vectors pre-digested with *EcoRI* and *XhoI*. Protein-protein interactions were tested in the yeast strain EGY48 according to the manufacturer's instructions. Oligos used for cloning of *SDF2*, *Erdj3B* and *BiP1* cDNAs are described in Supplementary Table III.

Protein co-immunoprecipitations

Protein co-immunoprecipitations were performed as described earlier (Moffett *et al*, 2002) using leaves of 5-week-old transgenic Arabidopsis plants using the anti-HA affinity matrix (Roche). Immunoprecipitates were analysed by western blot with anti-HA, anti-ERdj3B (Yamamoto *et al*, 2008), anti-SHD (Klein *et al*, 2006), anti-CRT (Pagny *et al*, 2000) and anti-BiP (Pedrazzini *et al*, 1997) antibodies (gifts from R Boston, S Nishikawa, and A Vitale).

Endo H assay

EFR-eGFP-HA and FLS2 were immunoprecipitated using the anti-GFP agarose (Caltag Medsystems), and protein G sepharose (Sigma) plus anti-FLS2 polyclonal antibodies (Chinchilla *et al*, 2007),

respectively. The treatment with Endo H (New England Biolabs) was performed for 1 h at 37°C according to the manufacturer's instructions.

Supplementary data

Supplementary data are available at *The EMBO Journal* Online (<http://www.embojournal.org>).

Acknowledgements

This research was supported by Biotechnology and Biological Sciences Research Council grant BB/F021046/1 (CZ), ERA-NET Plant Genomics (JDGJ, AM, BPHJT), the Gatsby Charitable Foundation (CZ, JDGJ), and Swiss National Foundation grant 31003A-120655 (DC). We thank A Jones and L Serazetdinova for their precious help with the mass spectrometry analysis, R Fuchs for his help with the confocal microscopy, D Alger and his team for excellent plant care, L Price and P Dominy for helpful advices on TAIL-PCR, and J Rathjen and R Strasser for their useful discussions and comments on the manuscript. R Boston, X Dong, B Kunkel, J Li, D Mackey, G Martin, B Mauch-Mani, J Molinier, S Nishikawa, and A Vitale are acknowledged for providing materials.

Conflict of interest

The authors declare that they have no conflict of interest.

References

- Anelli T, Alessio M, Bachi A, Bergamelli L, Bertoli G, Camerini S, Mezghrani A, Ruffato E, Simmen T, Sitia R (2003) Thiol-mediated protein retention in the endoplasmic reticulum: the role of ERp44. *EMBO J* **22**: 5015–5022
- Anelli T, Ceppi S, Bergamelli L, Cortini M, Masciarelli S, Valetti C, Sitia R (2007) Sequential steps and checkpoints in the early exocytic compartment during secretory IgM biogenesis. *EMBO J* **26**: 4177–4188
- Anelli T, Sitia R (2008) Protein quality control in the early secretory pathway. *EMBO J* **27**: 315–327
- Bies C, Blum R, Dudek J, Nastainczyk W, Oberhauser S, Jung M, Zimmermann R (2004) Characterization of pancreatic ERj3p, a homolog of yeast DnaJ-like protein Scj1p. *Biol Chem* **385**: 389–395
- Buck TM, Wright CM, Brodsky JL (2007) The activities and function of molecular chaperones in the endoplasmic reticulum. *Sem Cell Dev Biol* **18**: 751–761
- Chinchilla D, Zipfel C, Robatzek S, Kemmerling B, Nürnberger T, Jones JD, Felix G, Boller T (2007) A flagellin-induced complex of the receptor FLS2 and BAK1 initiates plant defence. *Nature* **448**: 497–500
- Clough SJ, Bent AF (1998) Floral dip: a simplified method for Agrobacterium-mediated transformation of Arabidopsis thaliana. *Plant J* **16**: 735–743
- Crofts AJ, Leborgne-Castel N, Pesca M, Vitale A, Denecke J (1998) BiP and calreticulin form an abundant complex that is independent of endoplasmic reticulum stress. *Plant Cell* **10**: 813–823
- Denecke J, Carlsson LE, Vidal S, Höglund AS, Ek B, van Zeijl MJ, Sinjorgo KM, Palva ET (1995) The tobacco homolog of mammalian calreticulin is present in protein complexes *in vivo*. *Plant Cell* **7**: 391–406
- de Torres M, Mansfield JW, Grabov N, Brown IR, Ammouneh H, Tsiamis G, Forsyth A, Robatzek S, Grant M, Boch J (2006) Pseudomonas syringae effector AvrPtoB suppresses basal defence in Arabidopsis. *Plant J* **47**: 368–382
- Ferrari S, Galletti R, Denoux C, De Lorenzo G, Ausubel FM, Dewdney J (2007) Resistance to Botrytis cinerea induced in Arabidopsis by elicitors is independent of salicylic acid, ethylene, or jasmonate signaling but requires PHYTOALEXIN DEFICIENT3. *Plant Physiol* **144**: 367–379
- Foresti O, De Marchis F, de Virgilio M, Klein EM, Arcioni S, Bellucci M, Vitale A (2008) Protein domains involved in assembly in the endoplasmic reticulum promote vacuolar delivery when fused to secretory GFP, indicating a protein quality control pathway for degradation in the plant vacuole. *Mol Plant* **1**: 1067–1076
- Gimenez-Ibanez S, Hann DR, Ntoukakis V, Petutschnig E, Lipka V, Rathjen JP (2009) AvrPtoB targets the LysM receptor kinase CERK1 to promote bacterial virulence on plants. *Curr Biol* **19**: 423–429
- Göhre V, Spallek T, Häweker H, Mersmann S, Mentzel T, Boller T, de Torres M, Mansfield JW, Robatzek S (2008) Plant pattern-recognition receptor FLS2 is directed for degradation by the bacterial ubiquitin ligase AvrPtoB. *Curr Biol* **18**: 1824–1832
- Gomez-Gomez L, Boller T (2000) FLS2: an LRR receptor-like kinase involved in the perception of the bacterial elicitor flagellin in Arabidopsis. *Mol Cell* **5**: 1003–1011
- Hann DR, Rathjen JP (2007) Early events in the pathogenicity of Pseudomonas syringae on Nicotiana benthamiana. *Plant J* **49**: 607–618
- Heese A, Hann DR, Gimenez-Ibanez S, Jones AM, He K, Li J, Schroeder JI, Peck SC, Rathjen JP (2007) The receptor-like kinase SERK3/BAK1 is a central regulator of innate immunity in plants. *Proc Natl Acad Sci USA* **104**: 12217–12222
- Hernández-Blanco C, Feng DX, Hu J, Sánchez-Vallet A, Deslandes L, Llorente F, Berrocal-Lobo M, Keller H, Barlet X, Sánchez-Rodríguez C, Anderson LK, Somerville S, Marco Y, Molina A (2007) Impairment of cellulose synthases required for Arabidopsis secondary cell wall formation enhances disease resistance. *Plant Cell* **19**: 890–903
- Hong Z, Jin H, Tzfira T, Li J (2008) Multiple mechanism-mediated retention of a defective brassinosteroid receptor in the endoplasmic reticulum of Arabidopsis. *Plant Cell* **20**: 3418–3429
- Jin H, Yan Z, Nam KH, Li J (2007) Allele-specific suppression of a defective brassinosteroid receptor reveals a physiological role of UGGT in ER quality control. *Mol Cell* **26**: 821–830
- Jin Y, Awad W, Petrova K, Hendershot LM (2008) Regulated release of ERdj3 from unfolded proteins by BiP. *EMBO J* **27**: 2873–2882
- Jin Y, Zhuang M, Hendershot LM (2009) ERdj3, a luminal ER DnaJ homologue, binds directly to unfolded proteins in the mammalian ER: identification of critical residues. *Biochemistry* **48**: 41–49
- Jones JD, Dangl JL (2006) The plant immune system. *Nature* **444**: 323–329
- Klein EM, Mascheroni L, Pompa A, Ragni L, Weimar T, Lilley KS, Dupree P, Vitale A (2006) Plant endoplasmic reticulum supports the protein secretory pathway and has a role in proliferating tissues. *Plant J* **48**: 657–673

- Koiwa H, Li F, McCully MG, Mendoza I, Koizumi N, Manabe Y, Nakagawa Y, Zhu J, Rus A, Pardo JM, Bressan RA, Hasegawa PM (2003) The STT3a subunit isoform of the Arabidopsis oligosaccharyltransferase controls adaptive responses to salt/osmotic stress. *Plant Cell* **15**: 2273–2284
- Li X, Lin H, Zhang W, Zou Y, Zhang J, Tang X, Zhou JM (2005) Flagellin induces innate immunity in nonhost interactions that is suppressed by *Pseudomonas syringae* effectors. *Proc Natl Acad Sci USA* **102**: 12990–12995
- Li X, Chu Z-H, Batoux M, Nekrasov V, Roux M, Chinchilla D, Zipfel C, Jones JDG (2009) Specific ER quality control components required for biogenesis of the plant immune receptor EFR. *Proc Natl Acad Sci USA* (e-pub ahead of print 26 August 2009; doi:10.1073/pnas.0905532106)
- Liu YG, Mitsukawa N, Oosumi T, Whittier RF (1995) Efficient isolation and mapping of Arabidopsis thaliana T-DNA insert junctions by thermal asymmetric interlaced PCR. *Plant J* **8**: 457–463
- Melotto M, Underwood W, Koczan J, Nomura K, He SY (2006) Plant stomata function in innate immunity against bacterial invasion. *Cell* **126**: 969–980
- Meskiene I, Baudouin E, Schweighofer A, Liwosz A, Jonak C, Rodriguez PL, Jelinek H, Hirt H (2003) Stress-induced protein phosphatase 2C is a negative regulator of a mitogen-activated protein kinase. *J Biol Chem* **278**: 18945–18952
- Meunier L, Usherwood YK, Chung KT, Hendershot LM (2002) A subset of chaperones and folding enzymes form multiprotein complexes in endoplasmic reticulum to bind nascent proteins. *Mol Biol Cell* **13**: 4456–4469
- Miya A, Albert P, Shinya T, Desaki Y, Ichimura K, Shirasu K, Narusaka Y, Kawakami N, Kaku H, Shibuya N (2007) CERK1, a LysM receptor kinase, is essential for chitin elicitor signaling in Arabidopsis. *Proc Natl Acad Sci USA* **104**: 19613–19618
- Moffett P, Farnham G, Peart J, Baulcombe DC (2002) Interaction between domains of a plant NBS-LRR protein in disease resistance-related cell death. *EMBO J* **21**: 4511–4519
- Molinier J, Ramos C, Fritsch O, Hohn B (2004) CENTRIN2 modulates homologous recombination and nucleotide excision repair in Arabidopsis. *Plant Cell* **16**: 1633–1643
- Nakagawa T, Kurose T, Hino T, Tanaka K, Kawamukai M, Niwa Y, Toyooka K, Matsuoka K, Jinbo T, Kimura T (2007) Development of series of gateway binary vectors, pGWBs, for realizing efficient construction of fusion genes for plant transformation. *J Biosci Bioeng* **104**: 34–41
- Nelson BK, Cai X, Nebenfuhr A (2007) A multicolored set of *in vivo* organelle markers for co-localization studies in Arabidopsis and other plants. *Plant J* **51**: 1126–1136
- Noh SJ, Kwon CS, Oh DH, Moon JS, Chung WI (2003) Expression of an evolutionarily distinct novel BiP gene during the unfolded protein response in Arabidopsis thaliana. *Gene* **311**: 81–91
- Pagny S, Cabanes-Macheteau M, Gillikin JW, Leborgne-Castel N, Lerouge P, Boston RS, Faye L, Gomord V (2000) Protein recycling from the Golgi apparatus to the endoplasmic reticulum in plants and its minor contribution to calreticulin retention. *Plant Cell* **12**: 739–756
- Pedrazzini E, Giovinazzo G, Bielli A, de Virgilio M, Frigerio L, Pesca M, Faoro F, Bollini R, Ceriotti A, Vitale A (1997) Protein quality control along the route to the plant vacuole. *Plant Cell* **9**: 1869–1880
- Ponting CP (2000) Novel repeats in ryanodine and IP3 receptors and protein O-mannosyltransferases. *Trends Biochem Sci* **25**: 48–50
- Queitsch C, Sangster TA, Lindquist S (2002) Hsp90 as a capacitor of phenotypic variation. *Nature* **417**: 618–624
- Reddy P, Sparvoli A, Fagioli C, Fassina G, Sitia R (1996) Formation of reversible disulfide bonds with the protein matrix of the endoplasmic reticulum correlates with the retention of un-assembled Ig light chains. *EMBO J* **15**: 2077–2085
- Rivas S, Rougon-Cardoso A, Smoker M, Schauser L, Yoshioka H, Jones JD (2004) CITRX thioredoxin interacts with the tomato Cf-9 resistance protein and negatively regulates defence. *EMBO J* **23**: 2156–2165
- Ruiz-Canada C, Kelleher DJ, Gilmore R (2009) Cotranslational and posttranslational N-glycosylation of polypeptides by distinct mammalian OST isoforms. *Cell* **136**: 272–283
- Saijo Y, Tintor N, Lu X, Rauf P, Pajerowska-Mukhtar K, Häweker H, Dong X, Robatzek S, Schulze-Lefert P (2009) Receptor quality control in the endoplasmic reticulum for plant innate immunity. *EMBO J* (e-pub ahead of print 17 September 2009)
- Schwessinger B, Zipfel C (2008) News from the frontline: recent insights into PAMP-triggered immunity in plants. *Curr Opin Plant Biol* **11**: 389–395
- Shan L, He P, Li J, Heese A, Peck SC, Nürnberger T, Martin GB, Sheen J (2008) Bacterial effectors target the common signaling partner BAK1 to disrupt multiple MAMP receptor-signaling complexes and impede plant immunity. *Cell Host Microbe* **4**: 17–27
- Shirasu K (2009) The HSP90-SGT1 chaperone complex for NLR immune sensors. *Annu Rev Plant Biol* **60**: 139–164
- Takai R, Isogai A, Takayama S, Che FS (2008) Analysis of flagellin perception mediated by flag22 receptor OsFLS2 in rice. *Mol Plant Micro Interact* **21**: 1635–1642
- Tedman-Jones JD, Lei R, Jay F, Fabro G, Li X, Reiter WD, Brearley C, Jones JD (2008) Characterization of Arabidopsis mur3 mutations that result in constitutive activation of defence in petioles, but not leaves. *Plant J* **56**: 691–703
- Tokunaga F, Brostrom C, Koide T, Arvan P (2000) Endoplasmic reticulum (ER)-associated degradation of misfolded N-linked glycoproteins is suppressed upon inhibition of ER mannosidase I. *J Biol Chem* **275**: 40757–40764
- van Esse HP, Van't Klooster JW, Bolton MD, Yadeta KA, van Baarlen P, Boeren S, Vervoort J, de Wit PJ, Thomma BP (2008) The Cladosporium fulvum virulence protein Avr2 inhibits host proteases required for basal defense. *Plant Cell* **20**: 1948–1963
- Vembar S, Brodsky JL (2008) One step at a time: endoplasmic reticulum-associated degradation. *Nat Rev Mol Cell Biol* **9**: 944–957
- Vitale A, Boston RS (2008) Endoplasmic reticulum quality control and the unfolded protein response: insights from plants. *Traffic* **9**: 1581–1588
- Wan J, Zhang XC, Neece D, Ramonell KM, Clough S, Kim SY, Stacey MG, Stacey G (2008) A LysM receptor-like kinase plays a critical role in chitin signaling and fungal resistance in Arabidopsis. *Plant Cell* **20**: 471–481
- Wang D, Weaver ND, Kesarwani M, Dong X (2005) Induction of protein secretory pathway is required for systemic acquired resistance. *Science* **308**: 1036–1040
- Williams DB (2006) Beyond lectins: the calnexin/calreticulin chaperone system of the endoplasmic reticulum. *J Cell Sci* **119**: 615–623
- Xiang T, Zong N, Zou Y, Wu Y, Zhang J, Xing W, Li Y, Tang X, Zhu L, Chai J, Zhou JM (2008) *Pseudomonas syringae* effector AvrPto blocks innate immunity by targeting receptor kinases. *Curr Biol* **18**: 74–80
- Yamamoto M, Maruyama D, Endo T, Nishikawa S (2008) Arabidopsis thaliana has a set of J proteins in the endoplasmic reticulum that are conserved from yeast to animals and plants. *Plant Cell Physiol* **49**: 1547–1562
- Zipfel C (2008) Pattern-recognition receptors in plant innate immunity. *Curr Opin Immunol* **20**: 10–16
- Zipfel C, Kunze G, Chinchilla D, Caniard A, Jones JD, Boller T, Felix G (2006) Perception of the bacterial PAMP EF-Tu by the receptor EFR restricts Agrobacterium-mediated transformation. *Cell* **125**: 749–760
- Zipfel C, Robatzek S, Navarro L, Oakeley EJ, Jones JD, Felix G, Boller T (2004) Bacterial disease resistance in Arabidopsis through flagellin perception. *Nature* **428**: 764–767